Pacific and Atlantic influences on Mesoamerican climate over the past millennium

D. W. Stahle · D. J. Burnette · J. Villanueva Diaz ·
R. R. Heim Jr. · F. K. Fye · J. Cerano Paredes ·
R. Acuna Soto · M. K. Cleaveland

Abstract A new tree-ring reconstruction of the Palmer Drought Severity Index (PDSI) for Mesoamerica from AD 771 to 2008 identifies megadroughts more severe and sustained than any witnessed during the twentieth century. Correlation analyses indicate strong forcing of instrumental and reconstructed June PDSI over Mesoamerica from the El Niño/Southern Oscillation (ENSO). Spectral analyses of the 1,238-year reconstruction indicate significant concentrations of variance at ENSO, sub-decadal, bi-decadal, and multidecadal timescales. Instrumental and model-based analyses indicate that the Atlantic Multidecadal Oscillation is important to warm season climate variability over Mexico. Ocean-atmospheric variability in the Atlantic is not strongly correlated with the June PDSI reconstruction during the instrumental era, but may be responsible for the strong multidecadal variance detected in the reconstruction episodically over the past millennium. June drought indices in Mesoamerica are negatively correlated with gridded June PDSI over the United States from 1950 to 2005, based on both instrumental and reconstructed data. Interannual variability in this latitudinal moisture gradient is due in part to ENSO forcing, where warm events favor wet June PDSI conditions over the southern US and northern Mexico, but dryness over central and southern Mexico (Mesoamerica). Strong anti-phasing between multidecadal regimes of tree-ring reconstructed June PDSI over Mesoamerica and reconstructed summer (JJA) PDSI over the Southwest has also been detected episodically over the past millennium, including the 1950–1960s when La Niña and warm Atlantic SSTs prevailed, and the 1980–1990s when El Niño and cold Atlantic SSTs prevailed. Several Mesoamerican megadroughts are reconstructed when wetness prevailed over the Southwest, including the early tenth century Terminal Classic Drought, implicating El Niño and Atlantic SSTs in this intense and widespread drought that may have contributed to social changes in ancient Mexico.

Keywords Mesoamerica · Montezuma baldcypress · Tree rings · PDSI · ENSO

D. W. Stahle (✉) · D. J. Burnette · F. K. Fye ·
M. K. Cleaveland
Department of Geosciences, University of Arkansas,
Ozark Hall 113, Fayetteville, AR 72701, USA
e-mail: dstahle@uark.edu

J. V. Diaz · J. C. Paredes
Laboratorio de Dendrocronologia, Instituto Nacional
de Investigacones Forestales, Agricolas, y Pecuarias,
CENID-RESPID Km 6.5 margen derecha canal Sacramento,
Gomez Palacio, Durango, Mexico
e-mail: villanueva.jose@inifap.gob.mx

R. R. Heim Jr.
National Climatic Data Center, NOAA, Asheville, NC, USA

R. A. Soto
Departamento Microbiologia y Parastologia, UNAM, Mexico,
D.F., Mexico
e-mail: yvonne@ibt.unam.mx

1 Introduction

Mexico is a semi-arid country with a history of serious socioeconomic impacts from extended drought and now faces the prospect of decreased precipitation, soil moisture, and stream flow with anthropogenic climate change (Meehl et al. 2007). Cool and warm season precipitation totals have both fluctuated significantly over Mexico during the twentieth and twenty-first centuries (Jauregui 1997; Seager et al. 2009; Stahle et al. 2009; Mendez and Magana 2010). The drought over northern Mexico during the 1990s and 2000s

curtailed stream discharge into Falcon Reservoir and Lake Amistad on the Rio Grande and heightened the international dispute between the US and Mexico over surface water supplies (Phillips 2002). In southern Mexico summer precipitation has declined significantly since 1940 (Douglas 2007; Stahle et al. 2009), but is important for recharge of the large reservoirs that supply 70% of the electrical power to Mexico City (de la Lanza-Espino and García Calderón 2002), one of the largest urban centers on Earth. Summer precipitation is also vital for subsistence agriculture across the highlands of Mexico where many native populations live in poverty and are still subject to climate-induced crop failure, hunger, and disease (Liverman 2000; Eakin 2000).

The precipitation climatology of Mexico is subject to a strong seasonal cycle and a steep latitudinal gradient (Wallen 1955; Mosiño and García 1974; Cavazos and Hastenrath 1990). The precipitation maximum occurs in summer over most of Mexico, and persistent drought over southern Mexico is often associated with wetness over northern Mexico and the southwestern US (Therrell et al. 2002; Mendez and Magana 2010). Modest cool season precipitation amounts over subtropical North America are often associated with "nortes" (the penetration of midlatitude frontal systems) and can be modulated in part by large-scale ocean-atmospheric forcing from the Pacific, especially by the El Niño/Southern Oscillation (ENSO). ENSO anomalies can influence Mexican climate during the cool season by modulating the Pacific-North American long wave circulation pattern and atmospheric dynamics associated with the subtropical jet stream (Trenberth et al. 1998; Seager et al. 2009). In central and southern Mexico, referred to here as Mesoamerica, summer precipitation is enhanced by the "temporales," which include episodic surges of moisture from the inter-tropical convergence zone (ITCZ) that bring increased precipitation into Central America, and by easterly waves from the Atlantic and Caribbean (Portig 1976; Pena and Douglas 2002; Mendez and Magana 2010). Warm season precipitation over Mesoamerica is teleconnected with SST anomalies in both the Pacific and Atlantic, with warm season drought favored by a warm tropical Pacific (El Niño) and a cold tropical Atlantic (Seager et al. 2009). El Niño conditions tend to enhance the Caribbean low-level jet (CLLJ), which suppresses the frequency of easterly wave activity and reduces warm season precipitation over Mesoamerica (Mendez and Magana 2010). On longer timescales, the Pacific Decadal Oscillation (PDO) and the Atlantic Multidecadal Oscillation (AMO) appear to impact persistent warm season (JJAS) moisture anomalies, including the latitudinal moisture gradient from southern to northern Mexico (Mendez and Magana 2010).

Long, high-resolution paleoclimatic data are limited in Mexico, but would have value for estimating the range of drought variability in the pre-instrumental period and for testing the strength of large-scale climate forcing from ENSO and other modes of ocean-atmospheric variability in the past. In this paper we analyze the climatic significance of the first millennium-long tree-ring reconstruction of annually-resolved moisture variability for central Mexico, previously published by Stahle et al. (2011) in a study of large megadroughts over Mesoamerica. We identify significant concentrations of variance in this new reconstruction that appear to be related to large-scale climate forcing of Mesoamerican climate emanating from the Pacific and Atlantic Ocean sectors. A number of high quality tree-ring reconstructions of past climate have already been developed for the US and northern Mexico (e.g., Cook et al. 2007). But the new reconstruction of the Palmer drought severity index (PDSI) is the first estimate for central Mexico that extends significantly earlier than the Colonial era, and it represents a distinctive regional climate province that responds differently to large-scale climate forcing from the tropical Pacific and Atlantic than is true farther north in Mexico and the southern United States. In fact, the warm season moisture balance over Mesoamerica tends to be anti-correlated with conditions over the central and southwestern US so the new reconstruction may help clarify the spatial patterns of moisture variability over North America and their cause. We describe interesting episodes of anti-phasing in tree-ring reconstructed multi-decadal regimes of drought and wetness between Mesoamerica and the southwestern US over the past millennium that may implicate large-scale ocean-atmospheric forcing.

2 Materials and methods

2.1 Chronology development

Barranca de Amealco is a steep-walled canyon cut into basalt near the continental divide between the Rio Panuco and Rio Lerma drainage systems in Queretaro (19.79°N, 91.03°W; Fig. 1), only 90 km north of Mexico City. Hundreds of centuries-old Montezuma baldcypress (*Taxodium mucronatum*) trees line the watercourse and many individual trees exceed 1,000-year of age (not all of which are solid or datable). The rural lands in the drainage basin surrounding Barranca de Amealco have been heavily developed for agriculture and grazing, but the ancient baldcypress trees along a 8 km reach have been protected by their remote location in the deep gorge.

The original tree-ring chronology for Barranca de Amealco and the derived June PDSI reconstruction were developed and described in Stahle et al. (2011). Core samples were extracted from the ancient trees at Amealco during ten separate field trips to the site over the period 2004–2009. The tree-ring series were dated under the microscope with
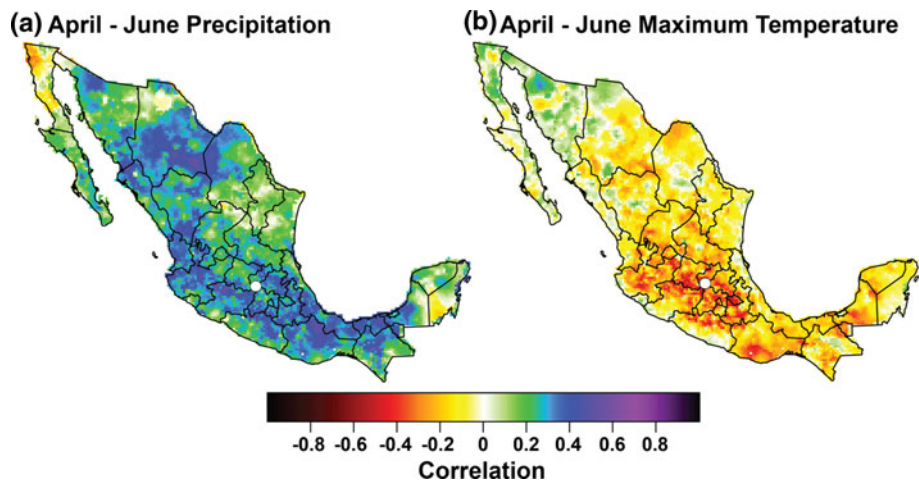
Fig. 1 The standard tree-ring chronology from Barranca de Amealco (*white dot*) is correlated for the 1950–2003 period with the 1/8° grid of monthly climate from Zhu and Lettenmaier (2007), after the monthly precipitation values were totaled for the April-June season (**a**) and averaged for April-June maximum temperature (**b**). The tree-ring chronology is strongly correlated with seasonal precipitation and maximum temperature over most of central and southern Mexico, indicating a strong response to available soil moisture

the skeleton plot and visual methods of crossdating (Douglass 1941; Stokes and Smiley 1996), augmented with segmented correlation analyses to ensure dating and measurement accuracy (Holmes 1983). The measured ring width series (0.001 mm precision) were non-stationary in the mean and variance and were detrended and standardized using the ratio of the fitted curve to the raw ring width values each year. A smoothing spline with a 50% frequency response equal to 100 years was used to standardize all series (Cook and Peters 1981). The final mean index chronology was computed with the ARSTAN program (Cook 1985; Cook and Holmes 1986) using robust estimation of the mean index value to discount statistical outliers. The internal consistency of the chronology over the entire 1,238-year time span was evaluated with the expressed population signal (EPS) statistic, which is a function of the mean correlation among the ring width series and sample size for a particular time segment of the chronology (Wigley et al. 1984). The variance of the final 1,238-year long chronology was stabilized with a 100-year spline to minimize the effect of sample size changes in the early portion of the record. Experimentation has shown that these detrending and variance stabilization procedures provide a reasonable solution to the differences in means and low frequency trends among the individual trees and radii from Barranca de Amealco, but have also removed multi-centennial variance that cannot be discriminated from long-term growth trend associated with increasing tree size and age.

2.2 Climate signal

The tree-ring chronology was correlated with gridded precipitation and temperature data available on a monthly basis

for Mexico to define the strongest seasonal and spatial climate signal recorded by the chronology during the instrumental era (Fig. 1). Zhu and Lettenmaier (2007) compiled a monthly precipitation and temperature dataset on a 1/8° grid over Mexico using station meteorological data maintained by the National Water Commission and other agencies in Mexico. The station data were screened for errors and outliers, and although the data begin in 1900 the highest quality and most spatially representative Mexican records are available only after 1950 (Jauregui 1997; Zhu and Lettenmaier 2007). Therefore, the tree-ring chronology was correlated with the gridded precipitation and temperature data from 1950 to 2003 to identify the monthly climate variables and region most suitable for reconstruction.

Paradoxically, baldcypress tree-ring chronologies in the United States and Mexico are in all cases directly correlated with precipitation and inversely correlated with temperature during the growing season, in spite of the frequently flooded site conditions (Stahle and Cleaveland 1992). This is the climate response typical of upland trees on moisture stressed sites. However, the fine feeder root systems of baldcypress trees tend to be stratified near the surface of the saturated soil or water column. Therefore, the positive baldcypress response to moisture availability appears to reflect both growth limitation during low water levels when these roots can be exposed to dry air, and growth enhancement during high waters when the roots are supplied with an increased flux of water with improved nutrient and dissolved oxygen levels (Stahle and Cleaveland 1992; Davidson et al. 2006).

Because the baldcypress chronology responds to both precipitation and temperature, the tree-ring chronology was also correlated with Palmer drought severity indices (PDSI;

Palmer 1965) using the new 0.5° gridded dataset that extends across North America from Canada through Mexico (Fig. 2). The PDSI is a soil moisture balance model indexed to regional climatology, where monthly precipitation represents the supply side of the balance and monthly mean temperature the demand side. A strong memory component is built into the PDSI, based on a Markovian persistence term of 0.897 from 1 month to the next (Cook et al. 2007). The integration of precipitation and temperature in the Palmer model of soil moisture provides a reasonable approximation for the climate forcing of tree growth and has been successfully used for tree-ring reconstructions of paleoclimate over North America and Asia (Cook et al. 2007, 2010). The gridded PDSI values were computed for the United States, Canada, and Mexico from a 0.5° gridded dataset of instrumental monthly temperature and precipitation observations, which was created from a high-quality suite of 5,639 temperature and 7,852 precipitation station records from North America. The station temperature data were treated for documented and undocumented change points, and outlier checks were applied to all station records. Climatologically-aided interpolation was used to grid the station data (Willmott and Robeson 1995).

Correlation analyses comparing the tree-ring chronology with the gridded monthly PDSI over North America were mapped to identify the seasonal and spatial climate signal embedded in the long Montezuma baldcypress tree-ring record (Fig. 2a illustrates the result for June PDSI). The

grid point data from the region with the strongest correlation against the baldcypress chronology were then extracted from the PDSI dataset, provided they were correlated at $r \geq 0.40$. This procedure resulted in the selection of 84 June PDSI 0.5° grid points from a rectangular latitude/longitude box over central and southern Mexico (the exact grid coordinates and all numerical data used in these analyses are available at http://www.uark.edu/dendro/Mesoamerica/cd.xls). These 84 locations were then averaged into an instrumental June PDSI time series for central Mexico (Fig. 3), representing the area of strongest correlations depicted in Fig. 2a and extending from Queretaro to Oaxaca, and Veracruz to Michoacan.

2.3 Calibration, verification, and analysis of the reconstruction

The standard ring-width chronology was calibrated with the instrumental June PDSI series for the central Mexico region using bivariate regression for a 31-year common period (1973–2003), after the predictor chronology and the predictand PDSI time series were each autoregressively (AR) modeled and prewhitened on the basis of the AR structure identified during the calibration period. Lead and lagged tree-ring variables were also considered as potential predictors in the regression modeling (i.e., tree-ring chronology values in year t_{+1} and t_{-1}), but they did not contribute additional skill in the estimation of June PDSI and were not used. The best autoregressive persistence model
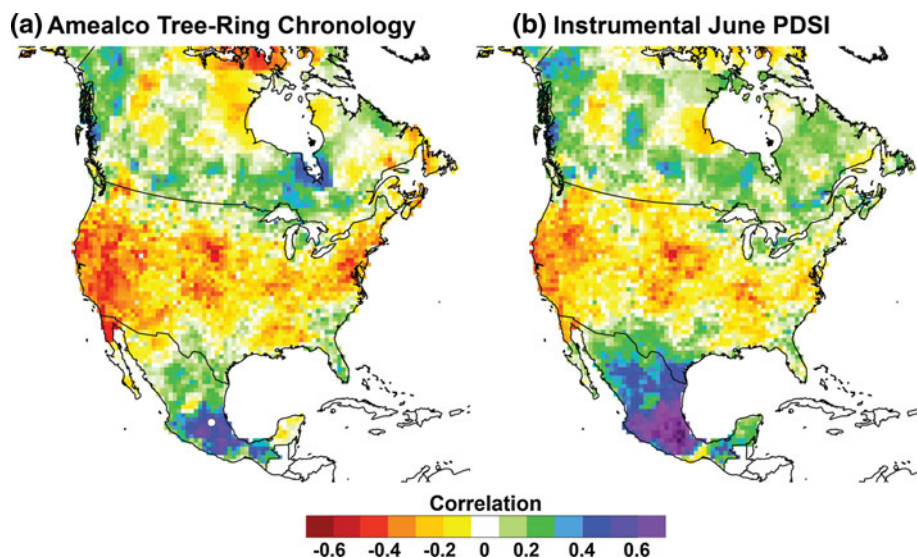

Fig. 2 **a** The standard tree-ring chronology from Amealco (*white dot*; after Stahle et al. 2011) and **b** the regional-average instrumental June PDSI based on 84 grid points in central Mexico are correlated with the gridded instrumental June PDSI compiled for North America from 1950–2005 (grid spacing is 0.5°). The regional average based on instrumental data is well correlated with grid points over central Mexico (**b**), as an average compared to its component grid points

must be. The strong positive correlation of the tree-ring chronology is more impressive because it is based on a single climate proxy and extends across the Mesoamerican cultural heartland (**a**). The broad field of negative correlations with June PDSI over the US (**a**, **b**) reflects the sharp latitudinal gradient in large-scale climate forcing that extends from tropical to temperate North America
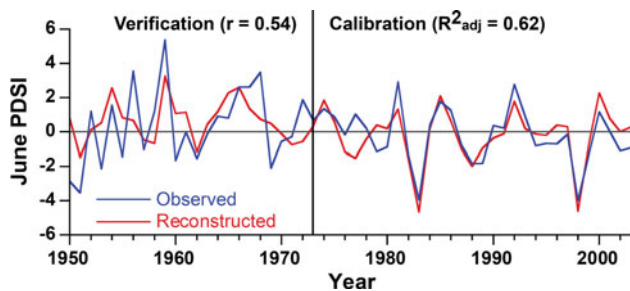
Fig. 3 The instrumental and tree-ring reconstructed June PDSI are plotted for central Mexico from 1950 to 2003 (after Stahle et al. 2011). The tree-ring data were calibrated with the instrumental data from 1973 to 2003 [adjusted R^2 and standard error of the regression estimates (=0.874) both based on whitened data] and were verified with instrumental PDSI not used for calibration from 1950 to 1972. Note the extreme droughts registered over central Mexico during the very strong El Niño events of 1983 and 1998. The slight negative trend in instrumental June PDSI over this time interval reflects in part the sharp rise in mean and maximum temperatures over central Mexico during the last 30 years (Cortez Vazquez 2006; Stahle et al. 2009)

for both time series was determined by computing the Aikaike Information Criterion with a correction for small sample bias [AR(2) coefficients of 0.2731 and −0.4484 for instrumental PDSI from 1973 to 2003 (mean = −0.1894), and AR(0) for the tree-ring chronology during this period (mean = 0.9002); c.f., Cook et al. 1999]. The AR model of the instrumental PDSI was added to the tree-ring estimates and the resulting reconstruction was then rescaled by the ratio of instrumental and reconstructed standard deviations for 1973–2003 to recover the variance lost in regression and thus complete the reconstruction (Fig. 4). The regression residuals of the calibration model were tested with the Durbin-Watson statistic (Draper and Smith 1981). The June PDSI data available for central Mexico from 1950 to 1972 were used to statistically test the accuracy of the calibration model on independent data (Cook et al. 1999).

To identify the strongest ocean-atmospheric forcing of the *early* warm season climate important to baldcypress growth, we correlated indices of ENSO, the PDO, NAO, and AMO with the gridded instrumental June PDSI over North America and Mexico (Fig. 5). The circulation indices were averaged during the boreal winter (DJF) when these modes of circulation tend to be most energetic, and the correlations were all computed for the 1951 to 2004 period. To examine joint ENSO and decadal scale variability during the instrumental era (e.g., Seager et al. 2010), we compute two indices to (1) emphasize the co-occurrence of warm ENSO events with the warm phase of the PDO (i.e., ENSO + PDO), and (2) to emphasize the combination of warm ENSO events with the cold or negative phase of Atlantic SSTs [i.e., ENSO-AMO]. These indices were computed as:

$$\text{ENSO} + \text{PDO} = \text{normalized DJF Nino3 year}_t + \text{normalized DJF PDO year}_t$$

$$\text{ENSO} - \text{AMO} = \text{normalized DJF Nino3year}_t - \text{normalized DJF AMO year}_t$$

Multi-taper spectral analysis (Mann and Lees 1996) was used to test the reconstruction for concentrations of variance at particular frequencies, and wavelet analyses were used to examine the temporal variability of frequency components (Grinsted et al. 2004).

3 Results

3.1 Reconstructed June PDSI for Mesoamerica

The derived tree-ring chronology for Barranca de Amealco is positively correlated with total precipitation and negatively correlated with maximum temperature during the spring-early summer (April-June) over most of Mexico, including the northern Yucatan Peninsula and Chihuahua (Fig. 1a, b). This classic moisture balance response is enhanced when the tree-ring chronology is correlated with the June PDSI, and the region of strongly positive correlations covers a large sector of Mesoamerica (Fig. 2a). The seasonal PDSI correlation of the Amealco chronology is concentrated in the early growing season (June), prior to the *canicula*, the mid-summer drought that typically occurs over central Mexico in July (Magana et al. 1999). Note that when the instrumental June PDSI series for central Mexico is correlated with the gridded instrumental June PDSI for North America, a pattern of positive correlations in Mexico and negative correlations across the central and southwestern US is produced, similar to the correlation results based only on the Amealco tree-ring chronology (Fig. 2 a, b). The spatial correlations in Fig. 2 are similar to the anticorrelation reported for warm season precipitation totals between western Mexico and the central US (Douglas et al. 1993; Higgins et al. 1997, 1999). Figure 2 also documents the impressive regional and large-scale climate signal encoded in the annual growth rings of the Mexican baldcypress trees, which is a function of both the strength of the climate signal recorded by the trees and the spatial autocorrelation of June PDSI over central Mexico.

The tree-ring chronology explains 62% of the variance in the instrumental PDSI data during the 1973–2003 calibration period ($R^2_{adj} = 0.62$, before re-reddening and rescaling; intercept = −0.0061, slope = 4.1249; Fig. 3), and the regression residuals are not significantly autocorrelated. During the 1950–1972 verification period, the Pearson correlation coefficient calculated between the instrumental and reconstructed June PDSI is $r = 0.54$ ($P = 0.004$), the

reduction of error (RE) is 0.32, and the coefficient of efficiency (CE) is 0.28. The derived tree-ring reconstruction of June PDSI for central Mexico is plotted from AD 771 to 2008 in Fig. 4a, along with smoothed versions emphasizing 10- and 30-year variability (Fig. 4b, c, respectively, based on smoothing splines used to filter the data with 50% frequency responses of 10-, and 30-year; Cook and Peters 1981). The EPS values for 100-year segments and the sample size of dated tree-ring specimens (radii) available for each year of the predictor chronology are also plotted in Fig. 4d, e. The EPS statistic remains at or above the 0.85 threshold, except for the first 100-year segment tested (771–870), when the sample size and internal consistency of the chronology decline even though the rings are correctly dated. The Amealco tree-ring chronology could also be calibrated and verified with early warm season precipitation totals (AMJ), but the statistics are uniformly lower than computed with June PDSI.

The Mexican PDSI data begin in 1895 and end in 2005, but the extracted regional average of June PDSI for the 84 grid points over central Mexico is not correlated with the reconstruction from 1895 to 1949 ($r = 0.03$). There is weak positive correlation with fewer individual grid points of June PDSI over the Queretaro region from 1895 to 1949, especially during the more recent 1923–1949 subperiod
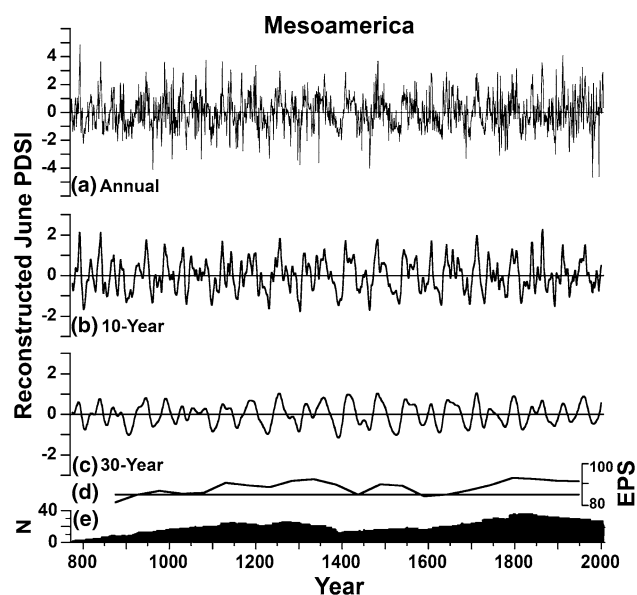

Fig. 4 Tree-ring reconstructed June PDSI for central Mexico is plotted from AD 771 to 2008, including the annual estimates (**a**), and smoothed versions emphasizing 10- (**b**) and 30-year variations (**c**). The EPS values for 100-year segments are plotted (**d**), along with the number of radii included in the predictor chronology each year (**e**). The estimates for 1983 and 1998 are the two lowest June PDSI values in the instrumental (1950–2003; Fig. 3) and reconstructed records (a, 771–2008), but the true reconstructed values for these two exceptionally dry years remain subject to biological, sampling, and statistical uncertainties

(not shown), and we suspect that the low correlations are primarily due to the sparse distribution of instrumental temperature and precipitation stations over Mexico during the early twentieth century (Jauregui 1997; Zhu and Lettenmaier 2007). Nevertheless, the strength of the climate signal recorded by the tree-ring chronology can also vary over time, as documented by the calibration and verification statistics.

The instrumental PDSI data for 2004 and 2005 were not used in the calibration because they reduce the quality of the regression model (e.g., R^2_{adj} declines from 0.62 to 0.51, autocorrelation increases in the residuals, and the estimation of 1983 and 1998, the two most extreme droughts of the instrumental record, is degraded). The reasons for this reduced skill are not known but may be related to sample size decline in the predictor chronology (Fig. 4e), undiscovered problems with the instrumental data, non-stationarity in the tree growth/climate relationship, or all of the above.

3.2 Drought extremes of 1983 and 1998

The instrumental and reconstructed June PDSI time series are well correlated from 1950 to 2003 (Fig. 3), even though the reconstruction is based on only a single tree-ring chronology from Queretaro, near the northern limit of the region used to compile the regional Mesoamerican drought index. The two most extreme observed and reconstructed droughts in central Mexico during the instrumental era occurred in 1983 and 1998 (Fig. 3, 1950–2003). These two severe Mexican droughts occurred during the El Niño events of 1982–1983 and 1997–1998, which were the strongest warm events in the 150-year instrumental record of the El Niño/Southern Oscillation (Federov and Philander 2000; McPhaden et al. 2006). Warm ENSO events tend to be associated with dry conditions during the summer season over Mesoamerica, and the 1983 and 1998 events were attended by profound drought and wildfire over both Mexico and Central America (Bell et al. 1999; Duncan et al. 2003).

The two most extreme single-year droughts in the entire 1,238-year reconstructed record are also estimated during the strong El Niño years of 1983 and 1998 (Fig. 4a). These extreme El Niño droughts might imply a recent increase in the intensity of warm ENSO events and associated climate impacts over Mesoamerica, potentially associated with warming in the eastern tropical Pacific (e.g., Hanson et al. 2006; Bunge and Clarke 2009). But both estimates occur near the end of the millennium-long series and their magnitude has been affected by the time series processing techniques used to develop the tree-ring chronology. Nonetheless, 1983 and 1998 were years of exceptionally

poor tree growth at Barranca de Amealco in spite of the statistical processing of the ring width data. The mean ring width value for 1998, without any detrending, indexing, robust estimation, variance adjustment, calibration, or rescaling is only 0.194 mm, which is the second lowest value in the 1,238-year simple mean ring width chronology (the lowest value occurred in 1466). The mean ring width for 1983 is just 0.385 mm, among the lowest 12% of all values in the chronology, and after 1600 (excluding the many low values in Medieval times) it was the second lowest mean ring width observed, second only to 1998. The simple mean ring width chronology does exhibit negative growth trend, associated with the increasing age and size of the trees, but that trend is steepest in the first 100- to 200-year of growth for most individual trees and the trend for the last few centuries of the mean ring width chronology is not sharply negative (not shown). While we doubt that 1983 and 1998 were truly the two most extremely dry June Palmer drought indices of the past 1,238 years as indicated in Fig. 4a, they were certainly extremely dry and may very well have been among the driest several years of the past millennium.

3.3 Large scale ocean-atmospheric forcing of early warm season climate over Mesoamerica

The climate of central and southern Mexico is strongly influenced by ENSO during the warm season (JJAS; Cavazos and Hastenrath 1990; Seager et al. 2009; Mendez and Magana 2010), particularly during El Niño events, but may also be modulated by other modes of circulation including the PDO (Pavia et al. 2006; Mendez and Magana 2010), the North Atlantic Oscillation (NAO, Fye et al. 2006), and the AMO (Sutton and Hodson 2005; Mendoza et al. 2007; Mendez and Magana 2010). There is strong latitudinal zonation in the ENSO teleconnection to June PDSI over North America during the 1951 to 2004 period (Fig. 5a). The Niño 3 index was used to represent ENSO variability and is negatively correlated with instrumental June PDSI over central and southern Mexico, indicating dry conditions during El Niño events (Fig. 5a). However, there is a strong positive correlation between the Niño 3 index and instrumental June PDSI over far northwestern Mexico and the southwestern US (Fig. 5a). The Niño 3 correlation with June PDSI is then negative again over a broad sector of the Pacific Northwest and southern Canada. These correlations reach -0.53 over southern Mexico, $+0.73$ over the Southwest, and -0.51 in British Columbia.

Instrumental June PDSI is also correlated with the PDO index, with a latitudinal pattern of negative and positive correlations similar to the Niño 3 teleconnection (Fig. 5b). However, the center of strongest positive correlation is shifted eastward into the southcentral US and northcentral Mexico (Fig. 5b). The June PDSI correlation with the NAO index is generally weaker than for Niño 3 or the PDO, and the strongest NAO response is detected from the lower Mississippi Valley into the northeastern US and southeastern Canada (Fig. 5c). The NAO correlations over Mexico are generally weak and inconsistent. The AMO exhibits a large area of negative correlation with June PDSI over northern Mexico and the southcentral US, with weak positive correlations over central and southernmost Mexico (Fig. 5d).

These instrumental analyses imply that a high-quality proxy of early warm season climate from central Mexico should encode evidence for climate forcing from both the Pacific and Atlantic Ocean sectors. The new June PDSI reconstruction for Mesoamerica is in fact significantly correlated with seasonal SST anomalies in the eastern equatorial Pacific, especially in the ENSO cold tongue region (Fig. 6). The reconstruction is also correlated with a pattern of SSTs in the North Pacific consistent with the spatial structure of the PDO, although the correlations are significant only in the subtropical northeast Pacific (not shown). These correlations were computed during the boreal cool season (DJFM) when El Niño events are normally strongest and initiate global scale responses in the coupled ocean atmospheric system, including drought over Mesoamerica during the following summer (Magana et al. 2003; Seager et al. 2009). The correlation was restricted to the 1931–2003 period, but the same correlation patterns exist in the Pacific prior to 1931, although they are weaker. Similar, though weaker correlation patterns were computed using instrumental June PDSI for central Mexico (not shown).

The correlations between observed and reconstructed June PDSI in central Mexico with Atlantic SSTs are much lower, and for the reconstruction are significant only in the western North Atlantic adjacent to Florida (Fig. 6). Nonetheless, the pattern of correlations with SSTs in the eastern equatorial Pacific and Gulf of Mexico-western North Atlantic is consistent with the forcing of warm season precipitation over Mesoamerica identified in observations and simulations (i.e., Mesoamerican drought during a warm tropical Pacific and cold Atlantic; Seager et al. 2009; Mendez and Magana 2010). A weaker version of this warm season response to Atlantic forcing is evident in the AMO correlations with June PDSI over southern Mexico (i.e., the *early* warm season; Fig. 5d).

Spectral analyses (Mann and Lees 1996) of the reconstruction indicate significant ($P < 0.01$) concentrations of variance a periods near 5.0, 7.4, 23.8, 31.9, and 62.1 years (Fig. 7), which might be linked with large-scale climate dynamics over Mesoamerica. Significant spectral power is detected in the nominal ENSO frequency band for periods from 3.6 to 5.8 years, peaking at 5.0 years. However,

Fig. 5 Instrumental Palmer drought indices for June at each grid point in the 0.5° data set for North America were correlated with indices of ENSO (the Niño 3 SST index; **a**), the PDO (**b**), NAO (**c**), and the AMO (**d**). All indices were obtained from the Climate Prediction Center of NOAA at http://www.noaa.gov/cpc/indices. The *circulation* indices were averaged for the DJF season, the correlations were computed for the 1951–2004 period, and the coefficients were mapped with GRASS Geographic Information System software
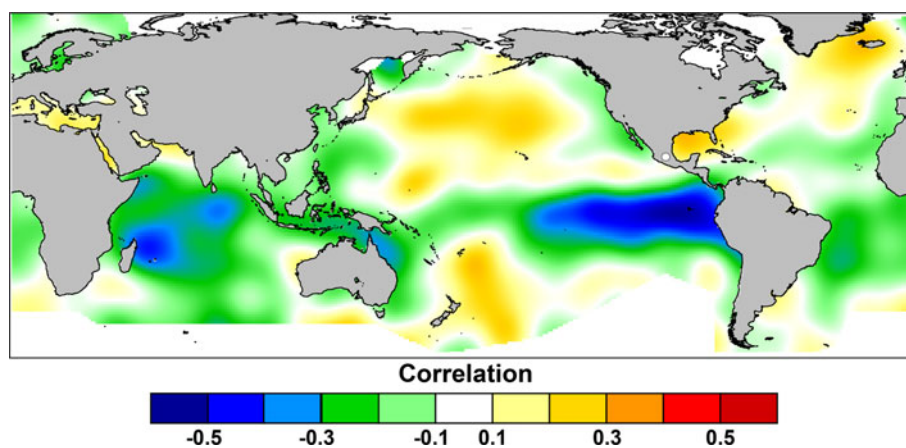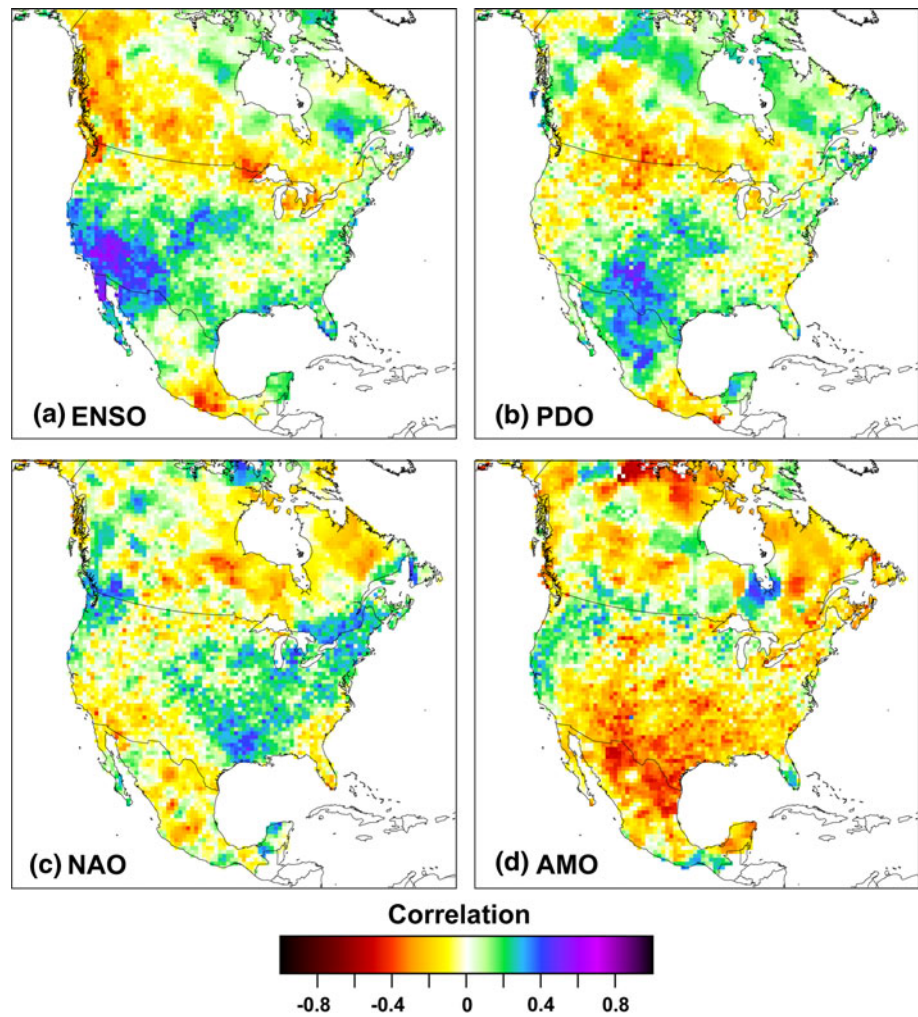

Fig. 6 The tree-ring reconstruction of June PDSI for central Mexico (chronology location = *white dot*) is correlated with global SSTs (Kaplan et al. 1998) during the boreal cool season (DJFM) for the period 1931–2003 (smoothed and mapped with GRASS software using a thin plate spline). The correlations in the cold tongue region of the eastern Pacific are significant ($P < 0.05$) and reach $r = -0.50$. The correlations in the North Pacific and North Atlantic are not significant except for small regions of positive correlation near Hawaii and Florida (*not outlined*)

wavelet analysis of the reconstruction indicates that variance in the ENSO band has been highly episodic over the past millennium, and was strongest during the twentieth century, late eighteenth century, and from approximately 900 to 1200 AD (Fig. 8). The presence of ENSO band variance during the relatively warm Medieval Period and during the twentieth century, and its absence during much of the Little Ice Age might suggest a link between global mean surface air temperature and ENSO forcing of Mesoamerican climate.

The NAO index of Jones et al. (1999) has a strong spectral peak at 7.78 years and may be linked with summer PDSI over the central United States and portions of eastern Mexico (Fye et al. 2006). The PDO may have a roughly 30-year timescale of variability (Labeyrie et al. 2003) and appears to modulate ENSO forcing of climate over Mexico (Mendez and Magana 2010). The NAO and PDO are plausible mechanisms for the spectral peaks observed in the reconstruction at periods of 7.4 and 31.9 years, but indices of the NAO and PDO are not correlated on an annual basis with the reconstruction during the instrumental era.

The frequency spectrum of reconstructed June PDSI is dominated by multidecadal variance that may be related to climate forcing from the Atlantic Ocean sector. Significant spectral power is detected at multidecadal timescales (50–75 years), peaking at 62.1 years (Fig. 7). However, wavelet analysis also indicates that the multidecadal power detected in the variance spectrum was not continuously present over the past millennium, and was significant from only approximately AD 1100 to 1600 (Fig. 8).

The Atlantic Multidecadal Oscillation might be implicated in the multidecadal variance in the June PDSI reconstruction. The reconstruction is not strongly correlated with SSTs in the North Atlantic (Fig. 6) or with
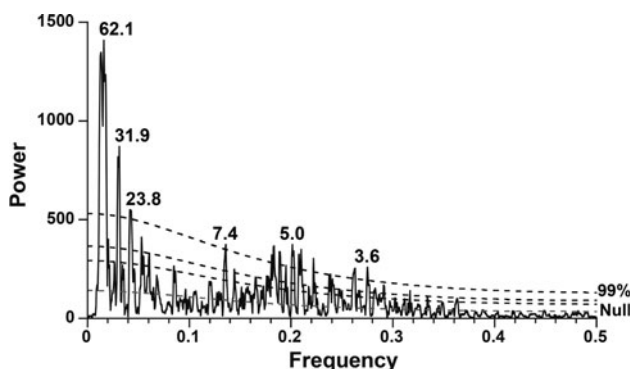

Fig. 8 The continuous wavelet power spectrum computed for the June PDSI reconstruction is illustrated from AD 771 to 2008. The strong power associated with significant wavelet variance is outlined by the heavy contour ($P < 0.05$), based on a red noise model (Torrence and Compo 1998; wavelet software from Grinsted et al. 2004). The edge of the wavelet area subject to uncertainty is shaded light gray. Note that significant wavelet power at periods between approximately 3- and 7-year has been highly episodic over the past millennium, and that multidecadal power was significant from approximately AD 1100 to 1600

seasonalized AMO indices during the instrumental era ($r = 0.06$; 1857–2003). But it is coherent ($P < 0.05$) at multidecadal frequencies with instrumental AMO indices during the mid-twentieth century when it emerges above the cone of influence (Torrence and Compo 1998). The phasing between the two series during the twentieth century is consistent with the positive correlation between the AMO and June PDSI, plus a seasonal lag between the preceding cool season AMO and June PDSI over Mexico. The reconstruction is also coherent with a tree-ring reconstruction of the AMO over the past 400 years (Gray et al. 2004) at periods variously between 16 and 75 years. But the phasing between the reconstructed AMO and reconstructed June PDSI in Mexico is inconsistent and only conforms with the expected phasing seen with the instrumental AMO in a relatively narrow frequency band near 50 years (cross wavelet coherence and phase were computed with software written by Grinsted et al. (2004), these coherency and phase spectra are not shown here, but are presented online at http://www.uark.edu/dendro/Mesoamerica/cd.xls). The June PDSI reconstruction is coherent with a tree-ring reconstruction of the NAO (Cook 2003) at periods between 60 and 70 years for a 200-year episode (AD 1450–1650), and the phasing is consistent with the positive correlation between the NAO index and June PDSI, along with a seasonal lag from the winter NAO to the June drought index.

Low frequency variations in Atlantic SSTs (i.e., the AMO) may be a reasonable hypothesis for the multidecadal power detected in the June PDSI reconstruction for Mesoamerica, based on these paleoclimatic results and the modern instrumental evidence for Atlantic influences on warm season climate over central Mexico (Sutton and

Fig. 7 Multi-taper method spectral analysis of the June PDSI reconstruction, AD 771–2008, using robust estimation and a red noise model for the null background variance ($2 \times 4\pi$ tapers; Mann and Lees 1996). Selected spectral peaks discussed in the text are annotated by period (in years). Significance thresholds are 90, 95, and 99%. The multidecadal component exceeds the 99% threshold for periods from 50 to 75 years
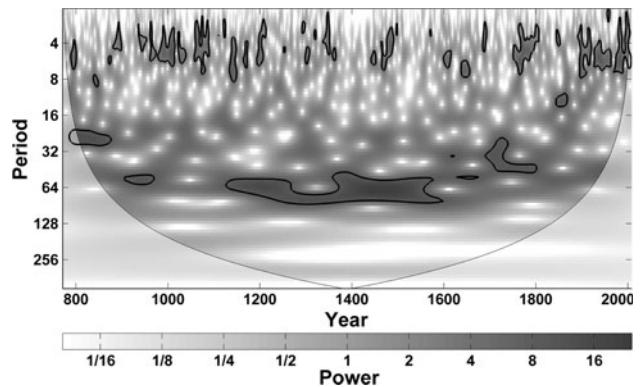
Hodson [2005](#); Seager et al. [2009](#); Mendez and Magana [2010](#)). However, multidecadal variability over Mesoamerica might also originate from the Pacific (Zhang et al. [1997](#); Gedalof and Smith [2001](#); Labeyrie et al. [2003](#)), perhaps ultimately orchestrated by interannual ENSO variability (Newman et al. [2003](#); Vimont [2005](#)). There are no major differences between the ENSO teleconnection to North American June PDSI when a combined ENSO + PDO index is used in the correlations, although the moisture response gradient from southern to northern Mexico is enhanced by the PDO influence (Figs. [5](#)a, b, [9](#)a). However, the June PDSI response to the combined ENSO-AMO index is stronger and more widespread over the southwestern US and northern Mexico than for either the ENSO or AMO indices alone (Figs. [5](#)a, d, [9](#)b). The moisture response gradient from southern to northern Mexico is also sharpened somewhat in the correlations with the joint ENSO-AMO index (Fig. [9](#)b), indicating that a warm eastern Pacific (El Niño) and cold Atlantic favor drought over Mesoamerica, but wetness over northern Mexico and the southwestern US.

Joint Pacific and Atlantic SST anomalies might therefore account for much of the interannual to multidecadal variability observed and reconstructed for the early warm season over Mesoamerica. However, when instrumental indices of the AMO and PDO are smoothed to emphasize multidecadal variability, the possible lower frequency relationship between the AMO index and reconstructed June PDSI during the instrumental era is not as strong as the multidecadal variability originating from the Pacific. The correlation between a 30-year smoothing of the June PDSI and the PDO is $r = -0.83$ for 1901–2004, but is only $r = 0.08$ for a 30-year smoothing of the AMO index from 1857 to 2005 [using a smoothing spline with a 50% frequency response of 30 years (Cook and Peters [1981](#)),

Fig. [10](#)a, b]. When a 60-year smoothing is applied to all series the correlation between the June PDSI reconstruction and the PDO is $r = -0.87$, but only $r = 0.28$ for the AMO. These joint analyses are necessarily restricted to the instrumental era, but nevertheless indicate that decadal variability in the Pacific may be more important than the Atlantic for low frequency moisture changes during the early warm season in Mesoamerica. However, multidecadal variability in the Atlantic may be more important in northern Mexico and the southwestern US because the smoothed AMO index is well correlated with smoothed JJA PDSI reconstruction for the Southwest ($r = -0.79$ and -0.84 for 30- and 60-year smooth time series, respectively; not shown).

3.4 Decadal variability in the moisture gradient between Mesoamerica and the southwestern United States

The June PDSI reconstruction identifies several prolonged droughts more severe and sustained than any witnessed during the modern instrumental era (Fig. [4](#)). These megadroughts were more prevalent prior to AD 1600 as has been identified by other paleoclimatic data from western North America (Stine [1994](#); Cook et al. [2004](#)). Prolonged multidecadal drought is reconstructed over central Mexico during the decline of Classic, Toltec, and Aztec civilizations and may have involved significant socioeconomic impacts (Stahle et al. [2011](#)). The Terminal Classic Drought in the early tenth century has been identified in lake sediment and speleothem proxies from Mexico (Hodell et al. [1995](#); Metcalfe et al. [2010](#); Medina-Elizalde et al. [2010](#)), but no high resolution evidence has previously been reported for the Toltec or Conquest era droughts in central Mexico centered at 1160 and 1520, respectively. Some of these

Fig. 9 a The gridded instrumental June PDSI data for North America are correlated with an index of Niño 3 SSTs and the PDO from 1950 to 2004. The index emphasizes the co-occurance of El Niño events with the warm phase of the PDO and La Niña events with the cold phase of the PDO. **b** As in a, but correlated with an index of the Niño 3-AMO, which emphasizes the co-occurrence of warm ENSO events and cold Atlantic SSTs
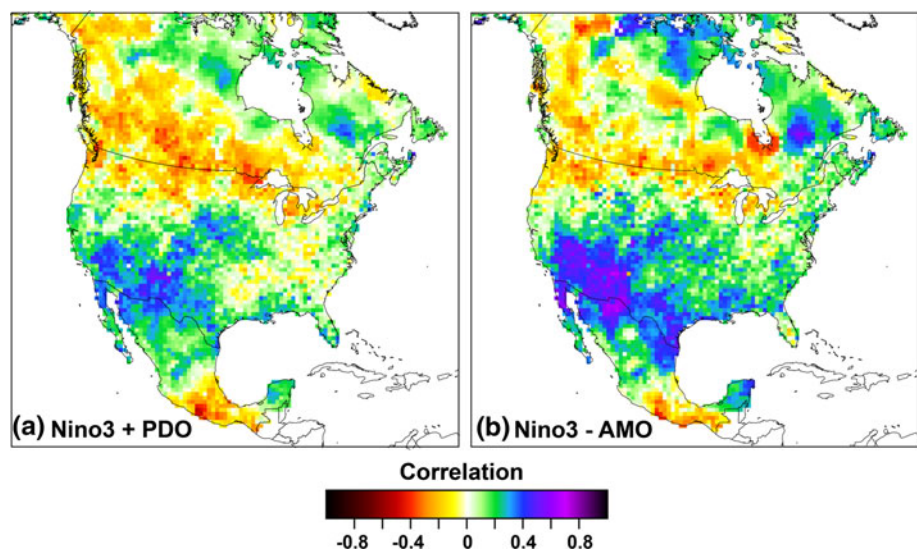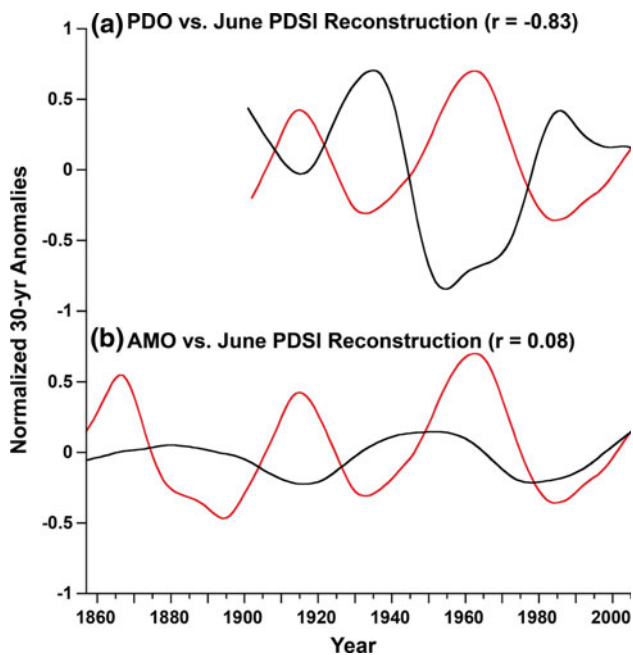
Fig. 10 **a** Tree-ring reconstructed June PDSI in Mesoamerica (*red*) and the winter PDO index (DJF, *black*) were both filtered to emphasize 30-year variability. The two series are strongly anti-correlated at this level of smoothing from 1901 to 2004 ($r = -0.83$). This decadal ENSO-like variability may be responsible for some of the anti-phasing between reconstructed June PDSI over Mesoamerica and summer PDSI in the Southwest (Fig. 11). **b** The smoothed tree-ring reconstructed June PDSI for Mesoamerica is compared with the smoothed AMO index (as in a, 1857–2004)

Mesoamerican megadroughts occurred during wet episodes over the southwestern US, and may implicate the large-scale ocean atmospheric forcing involved because El Niño events, perhaps augmented with decadal SST variability in the Pacific or Atlantic, favor drought over Mesoamerica simultaneously with wetness over the Southwest (Figs. 5, 9).

The reconstructed June PDSI for Mesoamerica is plotted with reconstructed summer (JJA) PDSI over the Southwest, after both were normalized and smoothed to emphasize 30-year variability (using a cubic spline with a 50% frequency response of 30-year; Cook and Peters 1981; Fig. 11). Some of the most severe decadal droughts reconstructed for Mesoamerica occurred during episodes of near normal to well above average moisture conditions in northern Mexico and the southwestern United States, including the deep and extended Mesoamerican droughts centered near AD 900, 1100, 1520, and 1690 (Fig. 11). Conversely, a few decadal pluvials occurred in Mesoamerica during reconstructed drought conditions farther north in the Southwest (centered near AD 990, 1250, 1350, 1640, 1860, and 1950; Fig. 11). Note that the JJA PDSI reconstructions for the Southwest (Cook et al. 2004) have a positive millennium-long trend of increasing soil moisture that has been linearly detrended for this comparison (before

normalization). This trend may largely reflect recovery from Medieval aridity, but other interpretations relating to changes in the geographical distribution and moisture versus temperature response of the longest available tree-ring chronologies dating back into Medieval times may also contribute to this trend and have not yet been thoroughly evaluated.

The Mesoamerican and southwestern US PDSI reconstructions are not correlated at the annual time scale ($r = -0.03$ from AD 771 to 2005; Fig. 11). Nonetheless, there is a tendency for single-year droughts to occur in the Southwest during wet extremes in Mesoamerica, and visa versa, based on a 5×5 contingency table analysis of the two regional reconstructions (Chi-square $P < 0.05$). This weak anti-phasing of single year extremes might reflect the latitudinal gradient in ENSO forcing of climate over Mexico and the Southwest, where warm events favor wetness in winter-spring over the Southwest but drought during spring-summer over Mesoamerica.

Even though the annual values of these two time series are not correlated, there is interesting anti-phasing of moisture regimes during the twentieth century contemporaneous with instrumental SST data that provides some constraint on the hypothesized ocean-atmospheric forcing
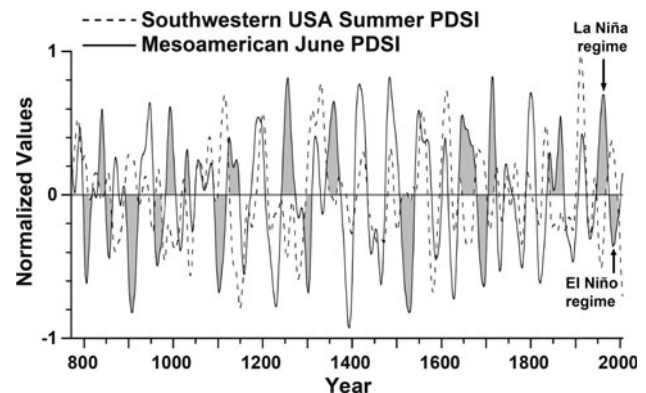

Fig. 11 The tree-ring reconstructed June PDSI for Mesoamerica is compared with the reconstructed summer (JJA) PDSI for a large region of the southwestern United States and extreme northern Mexico (roughly the region from the Pacific Coast to 100°W, and 30°–40°N, from the as yet unpublished 0.5° gridded reconstructions which update the analyses of Cook et al. 2004, 2007). Some of the most extreme multidecadal regimes of Mesoamerican drought occurred simultaneously with wet conditions of the Southwest, while several sustained Mesoamerican wet regimes occurred during Southwestern droughts (Mesoamerican droughts and pluvials that were out-of-phase with the Southwest shaded gray). Mesoamerican dryness in the 1980–1990s was matched by wetness in the Southwest and occurred during a regime of warm SSTs in the eastern Pacific and cold SSTs in the Atlantic ("El Niño regime"). Conversely, wet conditions in Mesoamerica in the 1950–1960s co-occurred with Southwestern drought, cold SSTs in the eastern Pacific, and a warm Atlantic ("La Niña regime"). Note also the episodes of *positive* correlation among PDSI regimes in the fifteenth, sixteenth, and early twentieth centuries

of the latitudinal moisture gradient. Mesoamerican June PDSI was relatively dry during the 1980–1990s when the Southwest was moist and warm events prevailed in the eastern Pacific while the Atlantic was cold ("El Niño regime" in Fig. 11; Wolter 2011). During the 1950–1960s the Southwest was dry and Mesoamerica was wet concurrent with a regime of cool SSTs in the eastern Pacific and warm SSTs in the Atlantic ("La Niña regime" in Fig. 11). A La Niña-like regime also appears to have prevailed during the mid-nineteenth century when Mesoamerican June PDSI was relatively wet and the Southwest was persistently dry (the so-called mid-nineteenth century or "Civil War Drought," Herweijer et al. 2006).

The comparison of smoothed reconstructions between Mesoamerica and the Southwest indicates approximately 10 multidecadal regimes with a latitudinal moisture gradient consistent with La Niña-like forcing, and another 10 regimes of anti-phasing consistent with El Niño-like forcing (Fig. 11). Notably, the early tenth century Terminal Classic Drought reconstructed for Mesoamerica was attended by above average moisture conditions in the Southwest. This large-scale latitudinal anti-phasing would be consistent with El Niño conditions in the eastern Pacific, perhaps amplified by a warm PDO condition and/or cooler than normal SSTs in the Atlantic (e.g., Seager et al. 2007; Mendez and Magana 2010). This hypothesis will need to be tested with very well dated and annually resolved proxies from the Pacific centers-of-action of ENSO, but it raises the intriguing possibility that the Terminal Classic Drought, and the decline of some Classic Period city states, were driven in part by a protracted regime of El Niño-like conditions.

It should be noted that the climate response of the tree-ring chronologies in the southwestern US and Mexico is not identical. Many Southwestern chronologies respond to climate during the winter-spring-early summer season (e.g., Fritts 1966), but the chronology from Queretaro responds primarily to spring-early summer (AMJ). Nevertheless, the sign of the instrumental moisture balance response to ENSO does switch between the cool and warm seasons over this region (Magana et al. 2003), as well as between the Southwest and central Mexico. So the latitudinal comparisons discussed here might be better than if the Mesoamerican chronology had the same climate response as seen in chronologies from the Southwest.

The most severe and sustained drought in the 1,200-year tree-ring reconstructions for western North America occurred in the mid-twelfth century (Cook et al. 2004; see also Fig. 11 for the Southwest). The onset of this epic drought occurred during a period of some 10 years when wetness prevailed in the smoothed Mesoamerican reconstruction, suggesting that frequent La Niña-like conditions and/or a cold PDO regime may have contributed to the

development of mid-twelfth century dryness over the Southwest. However, intense dryness developed in Mesoamerica before the mid-twelfth century drought abated in the Southwest and this large-scale latitudinal pattern of simultaneous drought may have contributed to the migrations and social unrest inferred during the decline of the Toltec state (Diehl 1983; Stahle et al. 2011).

One of the wettest episodes in the June PDSI reconstruction for Mesoamerica is estimated during the mid-thirteenth century (Fig. 11), an episode of long-term drought over the Southwest that finally culminated in the Great Pueblo Drought of the late thirteenth century identified in the first long tree-ring chronology ever developed (Douglass 1929). The Great Pueblo Drought ended by AD 1300 when intense drought developed Mesoamerica (Fig. 11), suggesting that El Niño-like conditions may have contributed to the alleviation of Ancient Puebloan drought during the early fourteenth century. The "17th Century Pueblo Drought" (Stahle and Dean 2011), which is reasonably well documented in historical records (Schroeder 1992), also appears to have occurred during a period of wetness over Mesoamerica (Fig. 11), implicating forcing from a La Niña-like regime.

Synchronous region-wide megadrought (i.e., dryness more severe and sustained than witnessed during the instrumental data) has not frequently impacted both the Southwest and Mesoamerica, but is apparent in the reconstructions during the mid-twelfth, early thirteenth, mid-fifteenth, and late nineteenth centuries (Fig. 11). The worst episode of simultaneous megadrought evident in the smoothed reconstructions occurred during the mid-fifteenth century, when drought prevailed over both regions from 1435 to 1473 (Fig. 11). This included the most extreme drought noted in the surviving pre-Hispanic Aztec codices, the "Drought of One Rabbit," lasting from at least 1452 to 1455 and attended by perhaps the worst famine in Aztec history (Therrell et al. 2004).

In addition to ENSO-like forcing of the latitudinal moisture gradient between tropical and temperate North America, persistent centennial-scale changes in the latitudinal position of the ITCZ have been reconstructed with marine sediments from the Caribbean Sea (Haug et al. 2001) and lake sediments from the tropical Pacific (Sachs et al. 2009), and might provide a model for some episodes of positive and negative phasing of moisture regimes between the Southwest and Mesoamerica. The most prolonged episode of in-phase multidecadal moisture regimes between these two regions occurred from ca. 1400 to 1640 (Fig. 11) when cold Northern Hemisphere conditions associated with the Little Ice Age may have suppressed the northern penetration of the ITCZ (Sachs et al. 2009), favoring more coherent region-wide climate variability over the Southwest and central Mexico. However, the tree-

ring chronology from Queretaro used to reconstruct June PDSI is located near the northern periphery of the Mesoamerican climate province (e.g., Fig. 2), so the paleoclimatic comparisons of the latitudinal moisture gradient presented in Fig. 11 will need to be strengthened with additional well dated, high resolution climate proxies from southern Mexico and Central America.

4 Discussion

The ancient Montezuma baldcypress trees found at Barranca de Amealco, Queretaro, preserve a long tree-ring record of environmental history that can be exactly dated and used to reconstruct the early growing season moisture balance over a large sector of central and southern Mexico for the past 1,238-year. Spectral analyses of the June PDSI reconstruction identify concentrations of variance at frequencies potentially associated with ENSO, the PDO, NAO, and AMO. The evidence for Pacific forcing of June PDSI at ENSO timescales is reasonable based on the modern ENSO teleconnection to both the observed and reconstructed moisture balance over Mesoamerica. But reconstructed variance in the nominal ENSO band (3–6 years) was highly episodic over the past millennium. ENSO band power was present in the reconstruction during the Medieval and modern eras, suggesting a possible link between ENSO forcing to Mesoamerica and a warmer background climate.

The evidence for Atlantic forcing of June PDSI over Mesoamerica rests on short instrumental observations of warm season climate anomalies during regimes of the AMO (Mendez and Magana 2010), climate model simulations of Atlantic forcing (Knight et al. 2006; Seager et al. 2009), significant spectral peaks in the reconstruction at sub-decadal and multidecadal timescales which may be related to the NAO and AMO, respectively, and the coherence between instrumental and reconstructed indices of the NAO and AMO at selected frequencies. The reconstruction is not significantly correlated with the NAO or AMO index during the instrumental era, but multidecadal regimes of Atlantic SSTs may have influenced reconstructed droughts and pluvials over Mesoamerica from AD 1100 to 1600 when the multidecadal frequency component constituted a large fraction of the variance in the reconstruction. If there were reliable observations of the AMO during the period from AD 1100 to 1600, then we could conduct a direct test of the hypothesis stating that reconstructed multidecadal variability in central Mexico June PDSI is related to Atlantic forcing. This is not possible now, but it might be in the future with further development of the high-resolution paleoclimate record.

The new reconstruction of June PDSI in Mesoamerica can be used with existing tree-ring reconstructions of summer PDSI over the Southwest to help document anomalies in the latitudinal moisture gradient between tropical and temperate North America. Strong north–south anti-phasing of multidecadal drought and wetness regimes has been identified at times over the past millennium, which may help fingerprint the large-scale forcing behind these regional climate anomalies. ENSO, or ENSO amplified by decadal SST anomalies in the North Pacific would be the leading suspect behind these regimes, given the strong teleconnections to North America in the instrumental era (although Atlantic SSTs may also be involved). When La Niña conditions, a cold PDO regime, and warm Atlantic SSTs prevailed in the 1950–1960s, the southwestern US suffered severe sustained drought, while above average June PDSI conditions prevailed in our reconstruction for Mesoamerica (Fig. 11). When El Niño conditions, a warm PDO regime, and cold Atlantic SSTs prevailed in the 1980–1990s, the Southwest registered above average wetness simultaneously with dry June PDSI conditions over Mesoamerica, especially during the extreme El Niño events of 1982–1983 and 1997–1998.

The most notable pre-instrumental example of anti-phasing appears to have occurred during the Terminal Classic Drought of the early tenth century, when severe sustained drought is reconstructed for Mesoamerican simultaneously with prolonged wetness over the Southwest. This steep latitudinal moisture gradient would be consistent with frequent El Niño conditions, a warm PDO regime, and a cold Atlantic. Because ENSO may actually orchestrate PDO variability in the North Pacific, and possibly some SST variability in the Atlantic, the El Niño phenomena may be implicated in some of the social changes that appear to have occurred among the Classic Period city states of ancient Mexico in the early tenth century.

Sixty years of tree-ring research have made it clear that millennium-old trees are extremely rare in Mexico and probably restricted to just one native species, Montezuma baldcypress (*T. mucronatum*). Just two Mexican forest locations have been proven to contain living trees more than 1,000-year old, Los Peroles in San Luis Potosi, and Barranca de Amealco, Queretaro (Villanueva Diaz et al. 2010). Only Amealco has provided an exactly dated millennium-long chronology thus far, and considering its strategic location in central Mexico, its valuable climate record, and its natural beauty, the undeveloped 8 km section of the barranca still lined with ancient baldcypress trees is a strong candidate for conservation. The dendrochronology of the ancient Montezuma baldcypress at Los Peroles has not yet been fully solved, although a replicated chronology has been exactly dated from AD 1350 to 2005 and a 700-year long floating chronology has been developed based on the crossdating among the inner rings on several very old trees, two of which are over 1,500-year old

based on simple ring counts. Baldcypress stands have recently been located on the Rio Nazas, Durango, and near Tzimol, Chiapas, with just a few trees at each location in the 800- to 1,000-year age class. Montezuma baldcypress is discontinuously distributed in Mexico (Martinez 1963), and other stands of ancient trees must still exist in this rugged and remote landscape. Given the interesting climate signals in the existing chronology from Barranca de Amealco, and the relevance of the June PDSI reconstruction to Mesoamerican climate dynamics and past cultural change, the discovery and development of millennium-long chronologies from additional ancient cypress trees in Mexico should be a priority for paleoclimatic research.

References

Bell GD, Halpert MS, Ropelewski CF, Kousky VE, Douglas AV, Schnell RC, Gelman ME (1999) Climate assessment for 1998. Bull Am Meteorol Soc 80:S1–S48

Bunge L, Clarke AJ (2009) A verified estimation of the El Niño index NINO3.4 since 1877. J Clim 22:3976–3992

Cavazos T, Hastenrath S (1990) Convection and rainfall over Mexico and their modulation by the Southern Oscillation. Int J Climatol 10:377–386

Cook ER (1985) A time series analysis approach to tree-ring standardization. Dissertation, Univ. of Arizona

Cook ER (2003) Multi-proxy reconstructions of the North Atlantic Oscillation (NAO) Index: a critical review and a new well-verified winter NAO Index reconstruction back to AD 1400. In: The North Atlantic oscillation: climatic significance and environmental impact, geophsycial monograph 134, Am Geophysical Union, pp 63–79

Cook ER, Holmes RL (1986) Users manual for program ARSTAN. Chronology series VI, University of Arizona

Cook ER, Peters K (1981) The smoothing spline: a new approach standardizing forest interior tree-ring series for dendroclimatic studies. Tree Ring Bull 41:45–53

Cook ER, Meko DM, Stahle DW, Cleaveland MK (1999) Drought reconstructions for the continental United States. J Clim 12:1145–1162

Cook ER, Woodhouse C, Eakin CM, Meko DM, Stahle DW (2004) Long-term aridity changes in the western US. Science 306:1015–1018

Cook ER, Seager R, Cane MA, Stahle DW (2007) North American drought: reconstructions, causes, and consequences. Earth Sci Rev 81:93–134

Cook ER, Anchukaitis KJ, Buckley BM, D'Arrigo R, Jacoby GC, Wright WE (2010) Asian monsoon failure and megadrought during the last millennium. Science 328:486–489

Cortez Vazquez J (2006) Mexico. In: Shein KA (ed) State of the climate in 2005. Bulletin of the American Meteorological Society, vol 87, pp S56–S57

Davidson GR, Laine BC, Galicki SJ, Threlkeld ST (2006) Root zone hydrology: why bald cypress in flooded wetlands grow more when it rains. Tree-Ring Res 62:3–12

de la Lanza-Espino G, García Calderón JL (2002) Historical summary of the geology, climate, hydrology, culture and natural resource utilization in the Basin of Mexico. In: Fenn E, de Bauer LI, Hernández-Tejeda T (eds) Urban air pollution and forest. Springer, Berlin, pp 3–23

Diehl RA (1983) Tula, the Toltec capital of ancient Mexico. Thames and Hudson, London

Douglas AV (2007) Summer precipitation variability over Mexico. AGU Joint Assembly, Acapulco, Mexico, May 2007

Douglas MW, Maddox RA, Howard K, Reyes S (1993) The Mexican monsoon. J Clim 6:1665–1667

Douglass AE (1929) The secret of the Southwest solved by talkative tree rings. Nat Geog 56:736–770

Douglass AE (1941) Crossdating in dendrochronology. J For 39:825–831

Draper NR, Smith H (1981) Applied regression analysis. Wiley, New York

Duncan BN, Martin RV, Staudt AC, Yevich R, Logan JA (2003) Interannual and seasonal variability of biomass burning emissions constrained by satellite observations. J Geophys Res 108. doi:10.1029/2002JD002378

Eakin H (2000) Smallholder maize production and climatic risk: a case study from Mexico. Clim Change 45:19–36

Federov AV, Philander SG (2000) Is El Niño changing? Science 288:1997–2002

Fritts HC (1966) Growth-rings of trees: their correlation with climate. Science 154:973–979

Fye FK, Stahle DW, Cook ER, Cleaveland MK (2006) NAO influence on sub-decadal moisture variability over central North America. Geophys Res Let 33:L15707

Gedalof Z, Smith DJ (2001) Interdecadal climate variability and regime-scale shifts in Pacific North America. Geophys Res Let 28:1515–1518

Gray ST, Graumlich LJ, Betancourt JL, Pederson GT (2004) A tree-ring based reconstruction of the Atlantic Multidecadal Oscillation since 1567 AD. Geophys Res Let 31:L12205. doi:10.1029/2004GL019932

Grinsted A, Moore JC, Jevrejeva S (2004) Application of the cross wavelet transform and wavelet coherence to geophysical time series. Nonlinear Proc Geophys 11:561–566

Hanson J, Sato M, Ruedy R, Lo K, Lea DW, Medina-Elizade M (2006) Global temperature change. Proc Nat Acad Sci 103:14288–14293

Haug GH, Hughen KA, Sigman DM, Peterson LC, Rohl U (2001) Southward migration of the intertropical convergence zone through the Holocene. Science 293:1304–1308

Herweijer C, Seager R, Cook ER (2006) North American droughts of the mid to late nineteenth century: a history, simulation and implication for medieval drought. Holocene 16:159–171

Higgins RW, Yao Y, Wang XL (1997) Influence of the North American monsoon system on the U.S. summer precipitation regime. J Clim 10:2600–2622

Higgins RW, Chen Y, Douglas AV (1999) Interannual variability of the North American warm season precipitation regime. J Clim 12:653–680

Hodell DA, Curtis JH, Brenner M (1995) Possible role of climate in the collapse of Classic Maya civilization. Nature 375:391–394

Holmes RL (1983) Computer-assisted quality control in tree-ring dating and measurement. Tree-Ring Bull 44:69–78

Jauregui E (1997) Climate changes in Mexico during historical and instrumental periods. Quat Int 43/44:7–17

Jones PD et al (1999) Monthly mean pressure reconstructions for Europe for the 1780–1995 period. Int J Clim 19:347–364

Kaplan A, Cane M, Kushnir Y, Clement A, Blumenthal M, Rajagopalan B (1998) Analyses of global sea surface temperature 1856–1991. J Geophys Res 103:18567–18589

Knight JR, Folland CK, Scaife AA (2006) Climate impacts of the Atlantic Multidecadal oscillation. Geophys Res Let 33:L17706

Labeyrie L et al (2003) The history of climate dynamics in the late quaternary. In: Alverson KD, Bradley RS, Pedersen TF (eds) Paleoclimate, global change and the future. Springer, Berlin, pp 33–61

Liverman DM (2000) Adaptation to drought in Mexico. In: Wilhite D (ed) Drought: a global assessment, vol 2. Routledge, New York, pp 35–45

Magana V, Amador JA, Medina S (1999) The midsummer drought over Mexico and Central America. J Clim 12:1577–1588

Magana V, Vazquez JL, Perez JL, Perez JB (2003) Impact of El Niño on precipitation in Mexico. Geofisica Int 42:313–330

Mann ME, Lees JM (1996) Robust estimation of background noise and signal detection in climatic time series. Clim Change 33:409–445

Martinez M (1963) Las Pinaceas Mexicanas. Universidad Nacional Autonoma de Mexio, Ciudad Universiteria, Mexico 20, D.F.

McPhaden MJ, Zebiak SE, Glantz MH (2006) ENSO as an integrating concept in earth science. Science 314:1740–1745

Medina-Elizalde M, Burns SJ, Lea DW, Asmerom Y, von Gunten L, Polyak V, Vuille Karmalkar A (2010) High resolution stalagmite climate record from the Yucatan Peninsula spanning the Maya terminal classic period. Earth Planet Sci Let 298:255–262

Meehl GA et al (2007) Global climate projections. In: Solomon S et al (eds) Climate change 2007: the physical science basis, contribution of working group I to the fourth assessment report of the intergovernmental panel on climate change. Cambridge University Press, Cambridge, pp 747–845

Mendez M, Magana V (2010) Regional aspects of prolonged meteorological droughts over Mexico and Central America. J Clim 23:1175–1188

Mendoza B, Garcia-Acosta V, Velasco V, Jauregui E, Diaz-Sandova R (2007) Frequency and duration of historical droughts from the 16th to the 19th centuries in the Mexican Maya lands, Yucatan Peninsula. Clim Change 83:151–168

Metcalfe SE, Jones M, Davies SJ, Noren A, MacKenzie A (2010) Climate variability over the last two millennia in the North American Monsoon region, recorded in laminated lake sediments from Laguna de Juanacatlan, Mexico. Holocene 20:1195–1206

Mosiño PA, García E (1974) The climate of Mexico. In: Bryson RA, Hare FK (eds) Climates of North America. Elsevier, New York, pp 345–404

Newman M, Compo GP, Alexander MA (2003) ENSO forced variability of the Pacific decadal oscillation. J Clim 16:3853–3857

Palmer WC (1965) Meteorological drought. Research Paper No. 45, US Dept Commerce, Weather Bureau

Pavia EG, Graef F, Reyes J (2006) PDO-ENSO effects in the climate of Mexico. J Clim 19:6433–6438

Pena M, Douglas MW (2002) Characteristics of wet and dry spells over the Pacific side of Central America during the rainy season. Mon Wea Rev 130:3054–3073

Phillips T (2002) Behind the U.S.-Mexico water treaty dispute. Interim News House Res Organ Texas House Represent 77(7):1–6

Portig W (1976) The climate of Central America. Climates of Central and South America. In: Schwerdtfeger H (ed) World survey of climatology, vol 12. Elsevier, Amsterdam, pp 405–478

Sachs JP, Sachse D, Smittenberg RH, Zhang Z, Battisti DS, Golubic S (2009) Southward movement of the Pacific intertropical convergence zone AD 1450–1850. Nat Geos 2:519–525

Schroeder AH (1992) Prehistoric Pueblo demographic changes. In: Vierra BJ (ed) Current research on the late prehistory and early history of New Mexico. Special Publication 1. New Mexico Archaeological Council, Albuquerque, pp 29–35

Seager R, Graham N, Herweijer C, Gordon LA, Kushnir Y, Cook E (2007) Blueprints for medieval hydroclimate. Quat Sci Rev 26:2322–2336

Seager R, Ting M, Davis M, Cane M, Naik N, Nakamura J, Li C, Cook E, Stahle D (2009) Mexican drought: an observational modeling and tree ring study of variability and climate change. Atmosfera 22:1–31

Seager R, Kushnir J, Nakamura J, Ting M, Naik N (2010) Northern hemisphere winter snow anomalies: ENSO, NAO and the winter of 2009/10. Geophys Res Let 37:L14703. doi:10.1029/2010 GL043830

Stahle DW, Cleaveland MK (1992) Reconstruction and analysis of spring rainfall over the Southeastern U.S. for the past 1000 years. Bull Am Meteorol Soc 73:1947–1961

Stahle DW, Dean JS (2011) North American tree rings, climatic extremes, and social disasters. In: Hughes MK, Swetnam TW, Diaz HF (eds) Dendroclimatology: progress and prospects. Developments in paleoenvironmental research, vol 11. Springer, Berlin, pp 297–327

Stahle DW, Cook ER, Villanueva Diaz J, Fye FK, Burnette DJ, Griffin RD, Acuna Soto R, Seager R, Heim RR Jr (2009) Early 21st century drought in Mexico. Eos 90(11):89–90

Stahle DW, Villanueva Diaz J, Burnette DJ, Cerano Paredes J, Heim RR Jr, Fye FK, Acuna Soto R, Therrell MD, Cleaveland MK, Stahle DK (2011) Major Mesoamerican droughts of the past millennium. Geophys Res Let 38:L05703. doi:10.1029/2010 GL046472

Stine S (1994) Extreme and persistent drought in California and Patagonia during medieval time. Nature 369:546–549

Stokes MA, Smiley TL (1996) An introduction to tree-ring dating, 2nd edn. University of Arizona Press, Tucson

Sutton RT, Hodson DLR (2005) Atlantic Ocean forcing of North American and European summer climate. Science 309:115–118

Therrell MD, Stahle DW, Cleaveland MK, Villanueva-Diaz J (2002) Warm season tree growth and precipitation over Mexico. J Geophys Res 107(D14):ACL 6-1 to 6-8

Therrell MD, Stahle DW, Acuna Soto R (2004) Aztec drought and the curse of one rabbit. Bull Am Meteorol Soc 85:1263–1272

Torrence C, Compo GP (1998) A practical guide to wavelet analysis. Bull Am Meteor Soc 79:61–78

Trenberth K, Branstator GW, Karoly D, Kumar A, Lau N, Ropelewski C (1998) Progress during TOGA in understanding and modeling global teleconnections associated with tropical sea surface temperate. J Geophys Res 103:14291–14324

Villanueva Diaz J, Ceranno Paredes J, Stahle DW, Constante Garcia V, Vazquez Salem L, Estrada Avalos J, de Dios Benadivdes S, Olorio J (2010) Ancient trees of Mexico. Revista Mexicana Ciencias Forestales 1(2):1–24

Vimont D (2005) The contribution of the interannual ENSO cycle to the spatial pattern of decadal ENSO-like variability. J Clim 18:2080–2092

Wallen CC (1955) Some characteristics of precipitation in Mexico. Geografiska Annaler 37:51–85

Wigley TML, Briffa KR, Jones PD (1984) On the average value of correlated time series, with applications in dendroclimatology and hydrometeorology. J Clim Appl Meteorol 23:201–213

Willmott CJ, Robeson SM (1995) Climatologically aided interpolation (CAI) of terrestrial air temperature. Int J Clim 15:221–229

Wolter K (2011) http://www.esrl.noaa.gov/psd/people/klaus.wolter/MEI/

Zhang Y, Wallace JM, Battisti DS (1997) ENSO-like interdecadal variability: 1900–1993. J Clim 10:1004–1020

Zhu C, Lettenmaier DP (2007) Long-term climate and derived surface hydrology and energy flux data for Mexico: 1925–2004. J Clim 20:1936–1946